Acta Mech
https://doi.org/10.1007/s00707-024-04058-y

ORIGINAL PAPER

Hadi Taibi · **Yahia Lasbet** · **Lakhdar Aidaoui**

Improving dynamic agitation by optimizing the localization of fins in an unsteady 2D chaotic mixer

Received: 3 March 2024 / Revised: 17 July 2024 / Accepted: 27 July 2024

Abstract The present paper investigates numerically the impacts of the addition of fins in 2D-unsteady chaotic micromixer on the dynamic behavior of fluid flow. Proposed designs are mainly based on the mounting of rigid fins on the constituted parts of the chaotic mixer. Fluid flow pattern is evaluated with the variance of the local properties presented in terms of velocity field, deformation and rotation rates, streamlines and elongation rate according to the proposed architectures. More precisely, the effects of three geometric configurations of the considered mixer are examined and compared. Findings illustrate that deformation and rotation rates are significantly improved with configuration 3 of the chaotic mixer protocol, where rotation phenomena create vortices of different sizes which improve mixing rate. In addition, configuration 3 enhances the elongation process responsible for fluid element stretching and folding, as continuous application of this transformation mixes the fluids in such geometry.

List of symbols

D	Deformation rate (s^{-1})
ε	Elongation rate
e	Eccentricity of rods (mm)
l	Length of fins (mm)
μ	Dynamic viscosity (Pa s)
Ω	Rotation rate (s^{-1})
Ω_t	Angular velocity of tank (rpm)
Ω_r	Angular velocity of rods (rpm)
P	Pressure (Pa)
ρ	Fluid density (kg m^{-3})
R	Outer tank radius (mm)
r	Rods radii (mm)
s	Surface (mm^2)
t	Time (s)
τ	Period of modulation (s)
U	Tangential velocity (mm s^{-1})
u, v	Velocity components (m s^{-1})
$\overrightarrow{V}$	Velocity field (m s^{-1})
ALT	Alternative

H. Taibi (✉) · Y. Lasbet · L. Aidaoui
Laboratory of Development in Mechanics and Materials, LDMM, Faculty of Sciences and Technology, University of Djelfa, Djelfa, Algeria
e-mail: h.taibi@univ-djelfa.dz

Published online: 27 August 2024

CM Continuous modulation

1 Introduction

Many engineering disciplines, including petroleum, pharmaceutical, environmental and food engineering, place a high priority on the topic of mass transfer and mixing [1–4]. When it comes to very viscous fluids, this subject is particularly challenging to overcome. As known, in laminar flow by considering the phenomena of chaotic advection, the chaotic mixing can be achieved. Furthermore, chaotic mixing is known to be the most effective mixing method when highly viscous fluids are concerned because chaotic advection flows can produce extremely intricate patterns of the advected scalar with strongly stretched structures and folded [5]. Numerous studies have been done to highlight the local characteristics of the velocity field at these kinds of flows and how they affect fluid mixing [6–9]. The relationship between chaotic mixing and the issue of the transfer of mass and heat is a topic that has received a lot of attention due to its evident industrial importance. In reality, this relationship is discussed in a large number of literary works. It is generally known that the convective factors in the equation of fluid motion play a significant role in the local properties of flows and have an impact on the local behavior of physical processes including deformation, rotation, stretching, and folding [10].

Mixers can be used in a wide range of industries and applications to blend different substances together where some general applications can be mentioned such as pharmaceutical, food and cosmetics industries. Besides, the type of fluids that can be mixed can vary widely, including liquids, powders, granules, semi-solids, and gases [11, 12]. The viscosity, density, and chemical properties of the fluids will determine the type of mixer and mixing process required for optimal blending.

Many different micromixer designs have been documented in the literature, and they can be divided into active and passive micromixers. Active mixers either use moving parts to create turbulent flows or an external power source such acoustics, pressure, magnetic field, and electric field [13–16], while the mixing process in passive mixers, which lack an additional forcing mechanism, is accomplished by altering their geometries to produce a transverse flow [17–19].

An efficient and simple way to raise these characteristics is by changing the geometric scale, as illustrated in the study of Lasbet et al. [20] where a numerical analysis is performed in order to evaluate the impact of the geometric scale on the fluid flow and its kinematic behavior. Local properties, such as dimensionless helicity contours, pressure losses, flow vortex stretching/folding coefficients, rotation rate, and deformation rate, were used to describe the fluid flow comportment. The obtained results show that decreasing the geometric scale is a key to enhancing the local physical process and thus heat transfer and fluid mixing in the studied geometry.

Moreover, in the creation of chaotic mixing, various flow geometries can be used, such as those that employ eccentric cylinders as rotational parts. For example, El Omari and Le Guer [21] examined numerically the development of two-dimensional mixing and the improvement of heat exchange within a two-rod stirring mechanism. It has been demonstrated by analyzing several stirring systems that have been used that non-continuous wall rotation helps to improve heat exchange through chaotic mixing. In a similar work of Ait Msaad et al. [22], a mixer made of rotating rods supported within a cylindrical tank was studied; the mixing performance and associated heating produced by chaotic advection are investigated using CFD simulations. In their study, Msaad et al. discussed how the number of revolving rods affects the mixer's thermal efficiency and chaotic advection. Findings revealed that the discontinuous wall cycles contribute to the improvement of the chaotic mixing and thus the improvement of the heat transfer. Saatdjian et al. [23] described a technique for analyzing the flow in a rotating, annular, and eccentric heat exchanger as well as a way for figuring out the ideal heat transfer parameters, namely ideal values for the eccentricity ratio and the rotating procedure that occurs periodically. From the results, it is well evident that in such continuous flows there is a frequency of cycle protocol where a maximum heat exchange rate is recorded.

The present study's goal is to evaluate the local physical parameters of the velocity field. Numerical research is done on a chaotic mixer with several proposed architectures. With the present numerical study, we aim to investigate the effect different geometrical configurations by adding fins on the components of chaotic mixer on local flow properties and kinematic behavior. More precisely, evaluate the variance of the presented fluid flow pattern in terms of velocity field, deformation and rotation rates, streamlines and elongation rate. To achieve this goal, different geometric configurations have been proposed and processed numerically in order to find out the optimal maneuvering leads to further instability of fluid flow.

2 Problem description

The present study aiming to use a simple geometry, consisting of rods and a tank with sine-squared angular velocity, generates a chaotic mixing flow. A comparative study is conducted to investigate several configurations by adding rigid fins on both the rods and the tank. The rotating mixer comprises a tank with a radius of $R = 50$ mm and two rods of equal radii ($r = 10$ mm) positioned with an eccentricity of $e = 10$ mm. Four different geometrical configurations are considered by adding fins of length $l = 10$ mm at various positions on the rods and the tank. In the present study, we consistently use the same rotation direction for the rods and for the outer tank. Specifically, the rods, with or without fins, rotate clockwise around their axis, while the tank rotates counterclockwise (Fig. 1). Two stirring protocols are considered for the time-modulation of angular velocity: continuous and non-continuous (see Table 1).

The maximal values of the angular velocities are set as: $\boldsymbol{\Omega_t} = 6\,\mathbf{rpm}$ for the outer tank, and $\boldsymbol{\Omega_r} = 30\,\mathbf{rpm}$ for the rods. In this case, the tangential wall velocity remains constant and equals to $\boldsymbol{U} = 31.41\,\mathbf{mm/s}$.

For the continuous protocol, the maximal angular velocity of the rods corresponds to the minimal of the outer tank and vice versa. In contrast, for the first half of the non-continuous modulation, the rods are stopped together while the outer tank is rotating, and for the second half, the opposite happens [2].

To enhance the impact of various rotation protocols on the characteristics of local flow and the kinematic behavior in the chaotic mixer, four geometrical configurations are proposed and studied numerically. The fluid inside the mixer is assumed to be Newtonian, viscous and incompressible. The density of the fluid under study is $\rho = 990\,\mathrm{kg/m^3}$, while its dynamic viscosity is $\mu = 1.5\,\mathrm{Pa\,s}$. The purpose is to compare the obtained results with those of the basic configuration (Configuration 1), which corresponds to the mixer without fins. In the second configuration, two fins are added vertically to the rods, while in the third configuration, four fins are

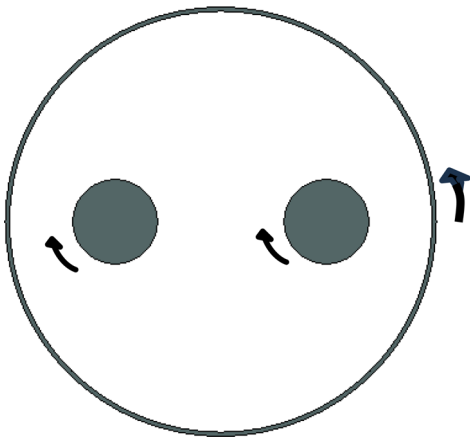

Fig. 1 Rotating mixer (basic configuration)

Table 1 The temporal modulation of the angular velocities of the rods and the tank [24]

Stirring protocol Component	Continuous	Non-continuous
Tank	$\Omega_t = 6 - 3\sin^2(\frac{\pi t}{\tau} + \frac{\pi}{2})$	$\Omega_t = 6 - 12\sin^2(\frac{\pi t}{\tau} + \frac{\pi}{2})$ If $\Omega_t < 0 \Rightarrow \Omega_t = 0$
Rods	$\Omega_r = 30 - 15\sin^2(\frac{\pi t}{\tau})$	$\Omega_r = 30 - 60\sin^2(\frac{\pi t}{\tau})$ If $\Omega_r < 0 \Rightarrow \Omega_r = 0$

Table 2 Considered grid sizes

Grid number	Number of elements
Grid 1	2966
Grid 2	14,848
Grid 3	55,188

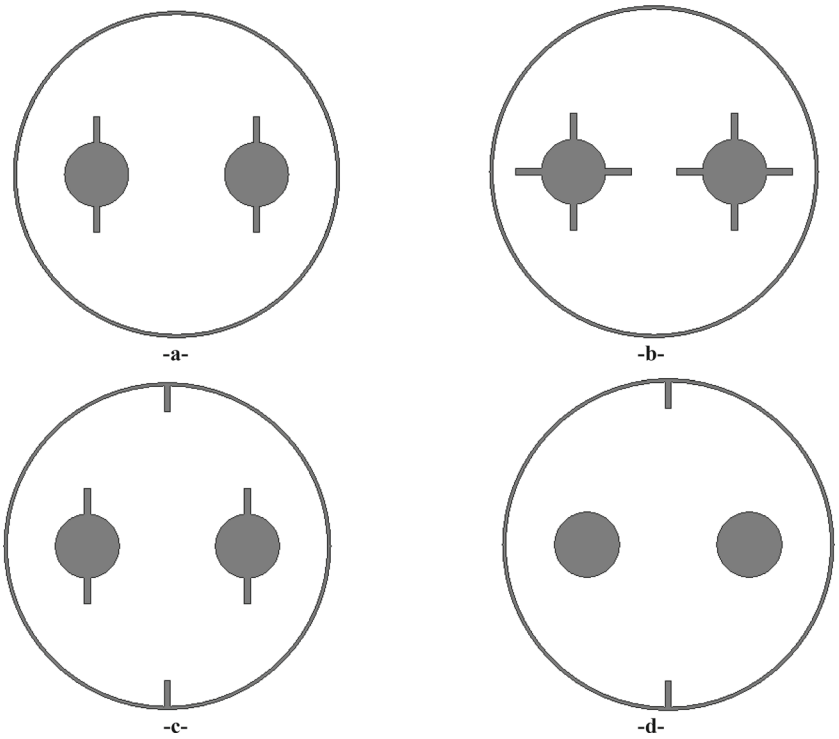

Fig. 2 Different proposed configurations: **a** Configuration 2: With fins on the rods, **b** Configuration 3: With double fins on the rods, **c** Configuration 4: With fins on the rods and on the tank, **d** Configuration 5: With fins on the tank

added (two vertically and two horizontally). The fourth configuration involves adding two fins vertically, one on the rod and the other on the outer tank. In the fifth configuration, the outer tank is supported by two vertically positioned fins. The proposed configurations are presented in the figures (Figs. 1, 2).

3 Mathematical formulation

The conservation equations of mass and momentum governing the unsteady laminar flow are shown as follow [25]:

The continuity equation:

$$\frac{\partial u}{\partial x} + \frac{\partial v}{\partial y} = 0 \tag{1}$$

Navier–Stokes equations in two flow directions (x and y):

$$\left(\frac{\partial u}{\partial t} + u\frac{\partial u}{\partial x} + v\frac{\partial u}{\partial y}\right) = -\frac{1}{\rho}\frac{\partial p}{\partial x} + \frac{\mu}{\rho}\left(\frac{\partial^2 u}{\partial x^2} + \frac{\partial^2 u}{\partial y^2}\right) \tag{2}$$

$$\left(\frac{\partial v}{\partial t} + u\frac{\partial v}{\partial x} + v\frac{\partial v}{\partial y}\right) = -\frac{1}{\rho}\frac{\partial p}{\partial y} + \frac{\mu}{\rho}\left(\frac{\partial^2 v}{\partial x^2} + \frac{\partial^2 v}{\partial y^2}\right) \tag{3}$$

Different parameters of the fluid flow are evaluated based on the considered configurations impact and compared with those of the basic configuration as discussed previously. The main parameters used to control the evolution of the consideration dynamic flow field are the deformation, rotation and elongation rates, presented as follows [26]:

- Deformation rate, presented by the next formula:

$$D = \frac{1}{S}\int\left(\left[2\left(\frac{\partial u}{\partial x}\right)^2 + 2\left(\frac{\partial v}{\partial y}\right)^2 + \left(\frac{\partial u}{\partial y} + \frac{\partial v}{\partial x}\right)^2\right]^{\frac{1}{2}}\right)ds \tag{4}$$

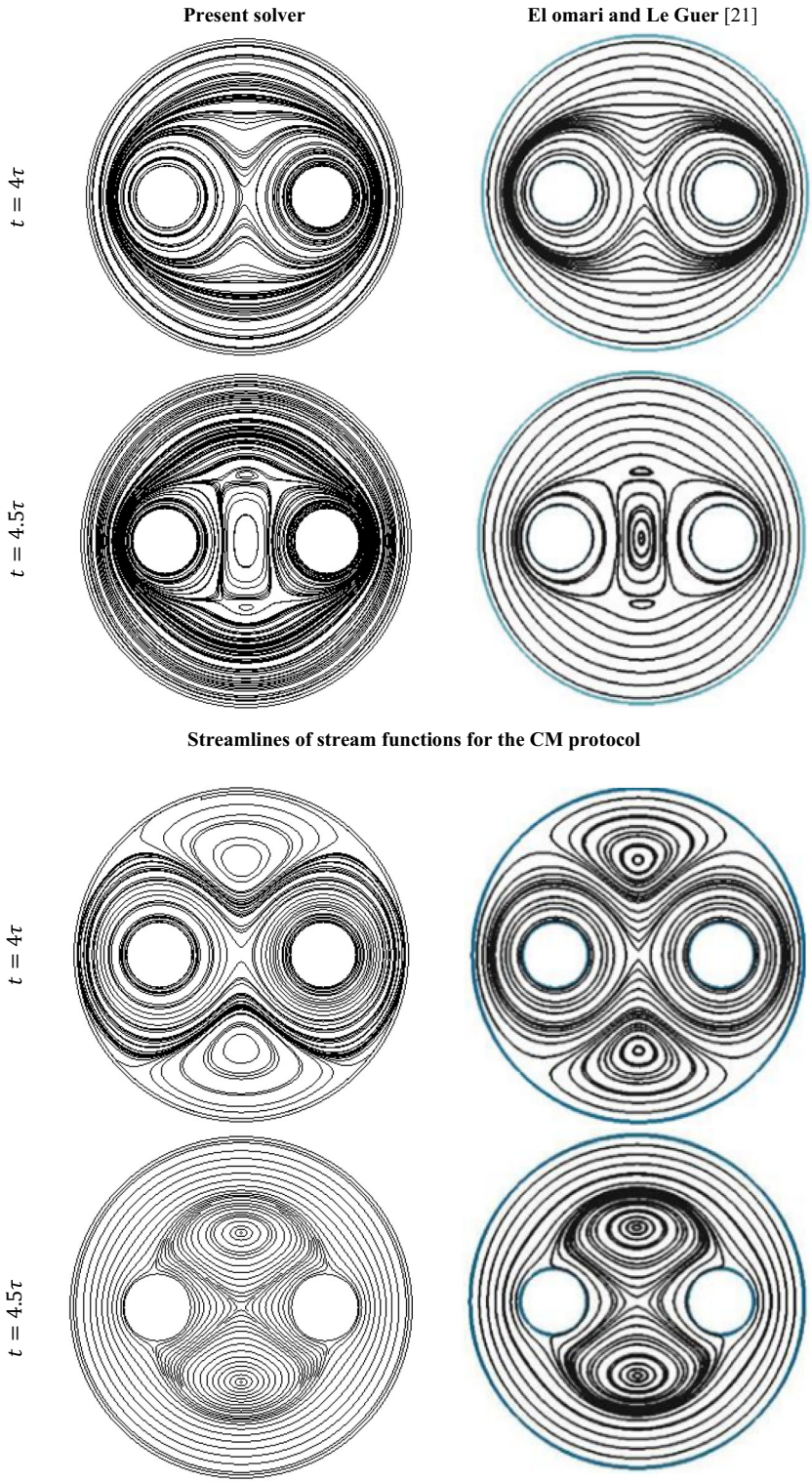

Fig. 3 Comparison of streamlines between present solver (left panel) and reference [21] (right panel) for the two stirring protocols

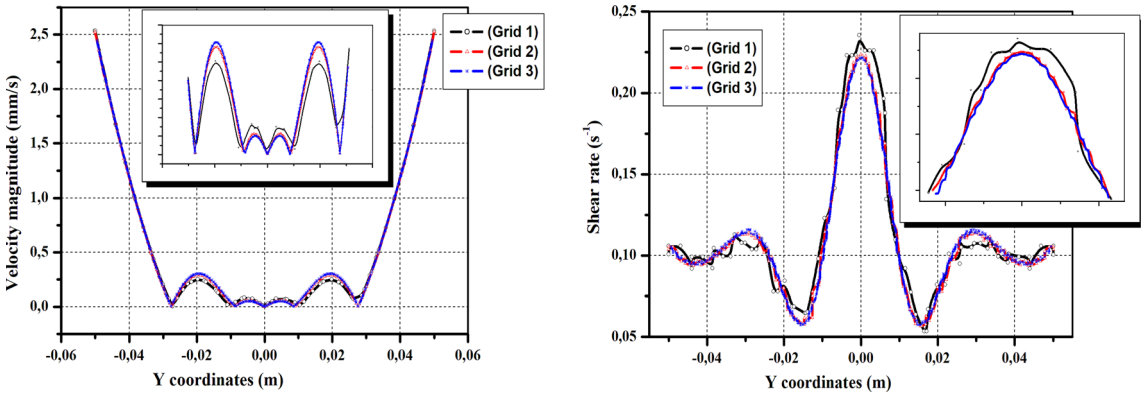

Fig. 4 Left side: Variation of velocity magnitude profiles with y-coordinates for various mesh densities at $t = 120$ s. Right side: Variation of shear rate with y-coordinates for various mesh densities at $t = 120$ s

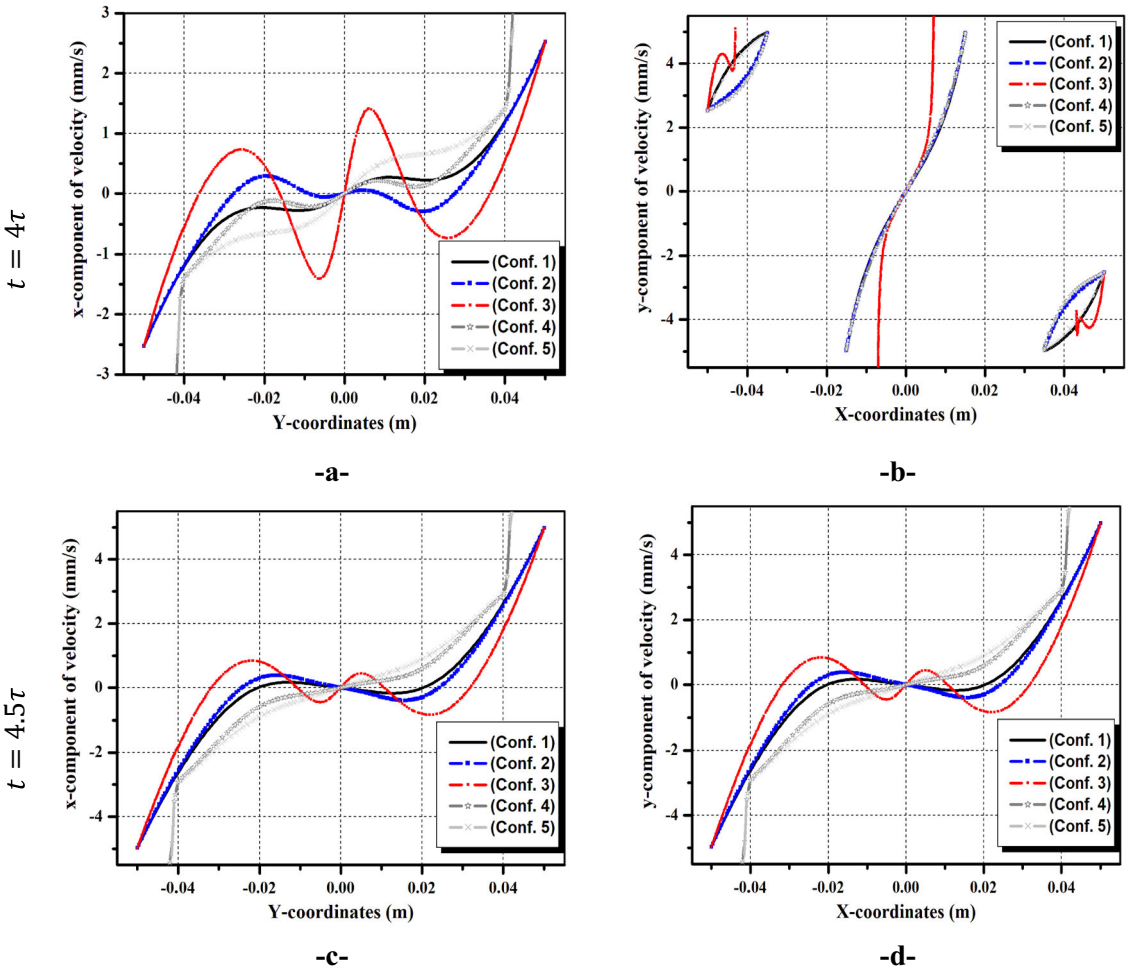

Fig. 5 Velocity components for the continuous modulation protocol (CM): **a** X-component versus y-coordinates at 120s; **b** Y-component versus x-coordinates at 120s; **c** X-component versus y-coordinates at 135s; **d** Y-component versus x-coordinates at 135s

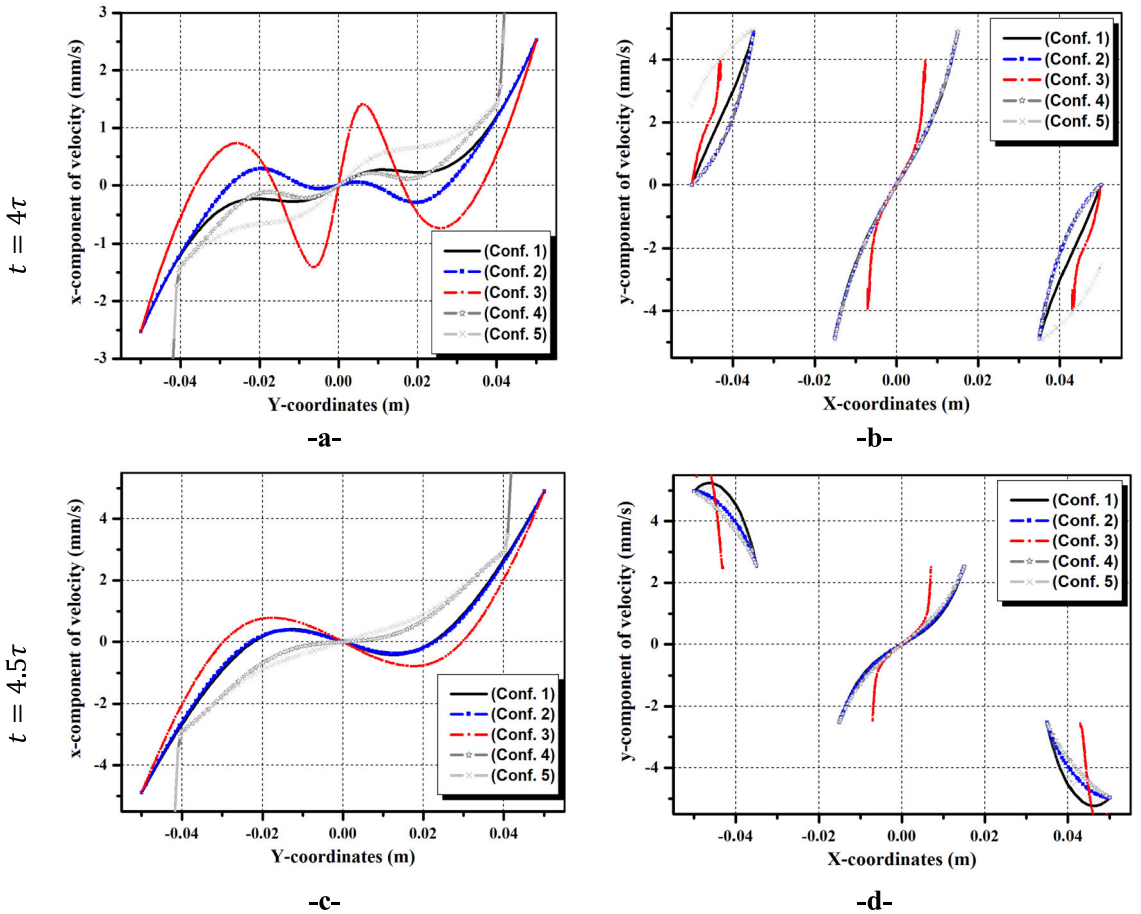

Fig. 6 Velocity components for the non-continuous modulation protocol (ALT): **a** X-component versus y-coordinates at 120s; **b** Y-component versus x-coordinates at 120s; **c** X-component versus y-coordinates at 135s; **d** Y-component versus x-coordinates at 135s

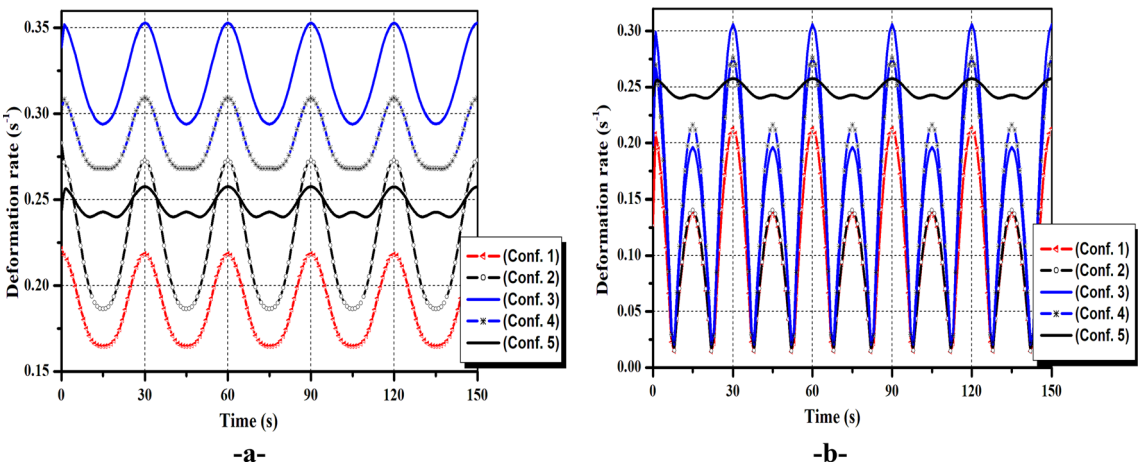

Fig. 7 Deformation rate versus time for various configurations using: **a** Continuous modulation protocol **b** Non-continuous modulation protocol

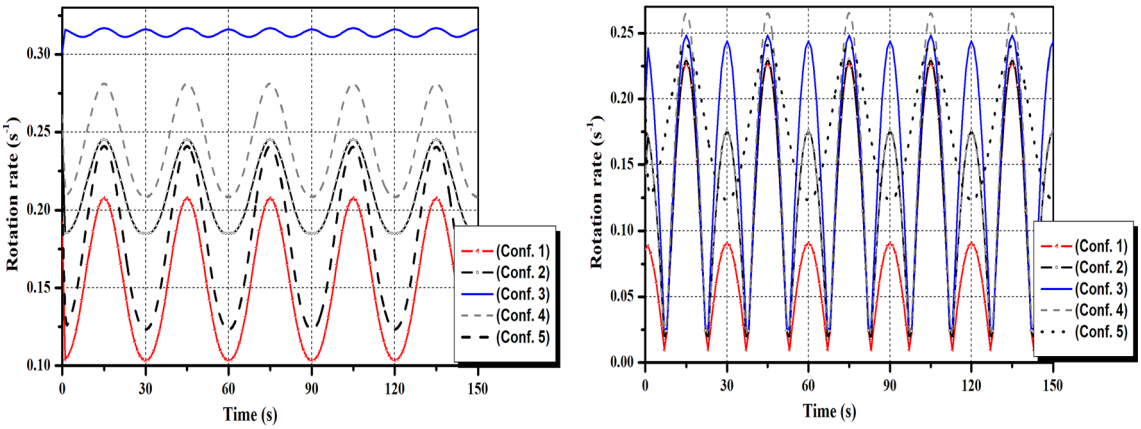

Fig. 8 Rotation rate versus time for various configurations using: **a** Continuous modulation protocol E.B **b** Non-continuous modulation protocol

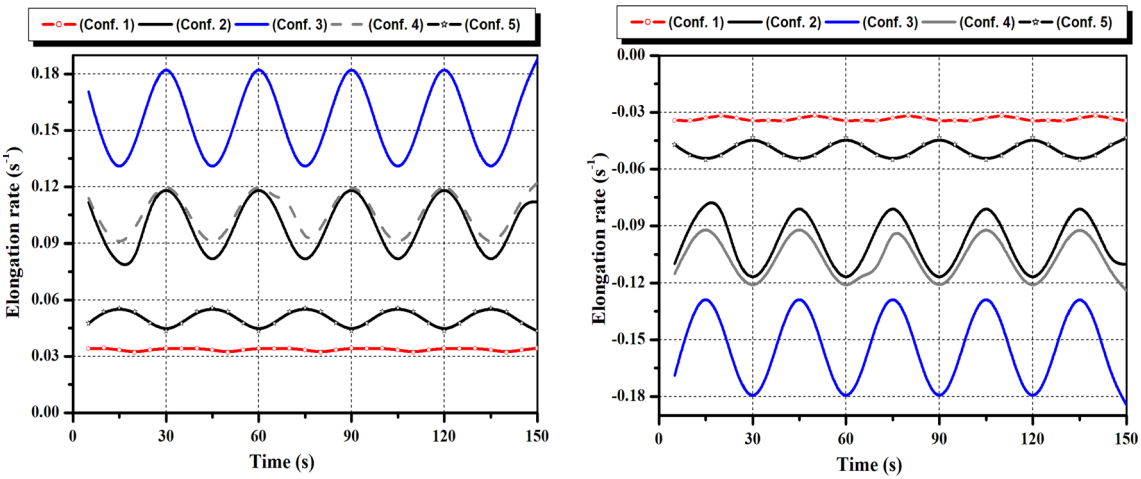

Fig. 9 Elongation rate versus time for various configurations using the continuous modulation protocol. **a** Positive elongation rates **b** Negative elongation rates

- Elongation rate, shown by the following equation:

$$\varepsilon = \frac{1}{S}\int\left(\frac{u^2\left(\frac{\partial u}{\partial x}\right)+v^2\left(\frac{\partial v}{\partial y}\right)+uv\left(\frac{\partial u}{\partial y}+\frac{\partial v}{\partial x}\right)}{u^2+v^2}\right)ds \tag{5}$$

- Rotation rate defined as:

$$\Omega = \frac{1}{S}\int\left(\frac{1}{2}\left|\frac{\partial v}{\partial x}-\frac{\partial u}{\partial y}\right|\right)ds \tag{6}$$

4 Validation

In order to ensure the accuracy and reliability of the numerical simulations performed by the used CFD code, some results are compared with the literature. Therefore, two specific instances $t = 120$ s and $t = 135$ s are selected for comparison, focusing on key time points that were previously analyzed and reported in the literature. The streamlines of the stream functions obtained from the numerical simulations are carefully

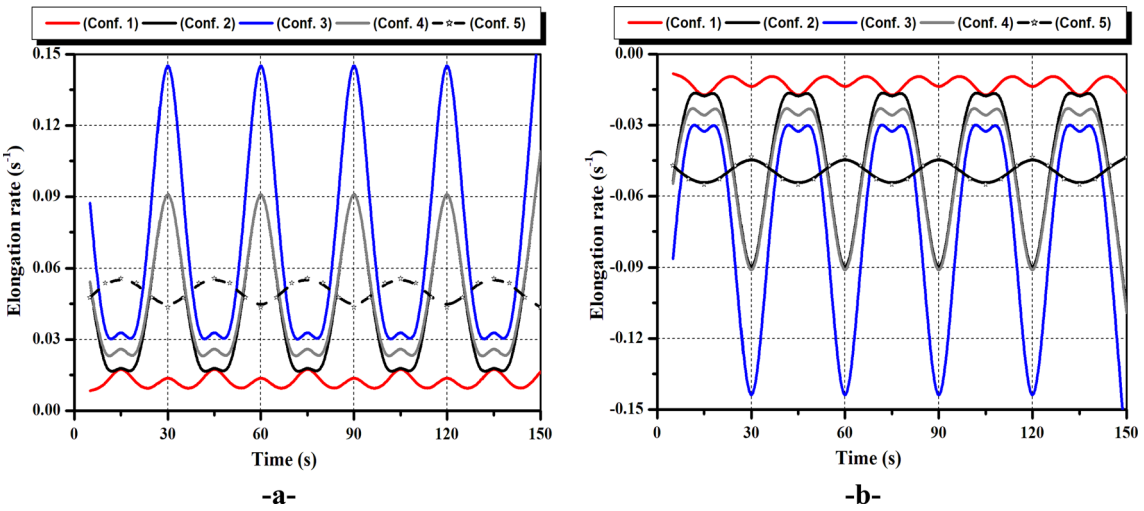

Fig. 10 Elongation rate versus time for various configurations using the non-continuous modulation protocol. **a** Positive elongation rates **b** Negative elongation rates

analyzed and compared with the corresponding streamlines from the literature (El Omari and Le Guer [21]) to achieve the qualitative agreement in the flow patterns, including the shape and distribution of streamlines. Additionally, quantitative measures, such as vortex size, flow recirculation regions, and overall flow patterns, are taken into account for a comprehensive validation analysis.

Indeed, as depicted in Fig. 3, the results from the current study exhibit a notable qualitative agreement with those reported in the literature. This agreement provides a robust validation for the accuracy and reliability of our numerical simulations.

5 Mesh study

In order to evaluate grid independence and find the best compromise between accuracy and computational cost, a mesh study is conducted. The sensitivity of the solution to changes in mesh size is tested by comparing the numerical results obtained from three different meshes: grid1, grid2 and grid3, each with increasing sizes as mentioned in Table 2.

The comparison focused on analyzing the velocity magnitude and the shear rate at a specific moment ($t =$ 120 s) in the basic configuration with continuous modulation.

It is evident from Fig. 4 that the results obtained using grid2 closely match those obtained from grid3, despite the latter having a finer mesh. This indicates that grid2 is capable of providing accurate and reliable results. Therefore, grid2 is adopted as the mesh for the problem under investigation. The chosen grid corresponds to a mesh with 14,848 of elements. In addition, the moving mesh technique is employed to simulate the fluid flow in consideration, as it allows for the adaptation of the mesh to accommodate the changing shape of the domain caused by boundary motion.

6 Results and discussion

The flow that is the subject of this study is complex from a temporal point of view in both CM and ALT protocols. The temporal disturbance makes the flow kinematically chaotic. A priori, the insertion of the fins in this flow adds geometric complications which will then considerably influence the hydrodynamic behavior of the velocity field which will subsequently increase the level of chaoticity. The proposed configurations are compared to the base case where the fins are not taken into consideration. The parameters considered are the velocity profile, rates of deformation and rotation, elongation rate, and streamlines.

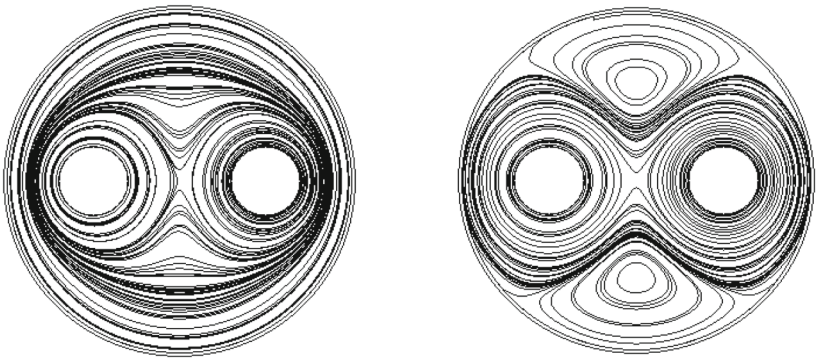

Configuration 1 : Rotating mixer without fins (base configuration)

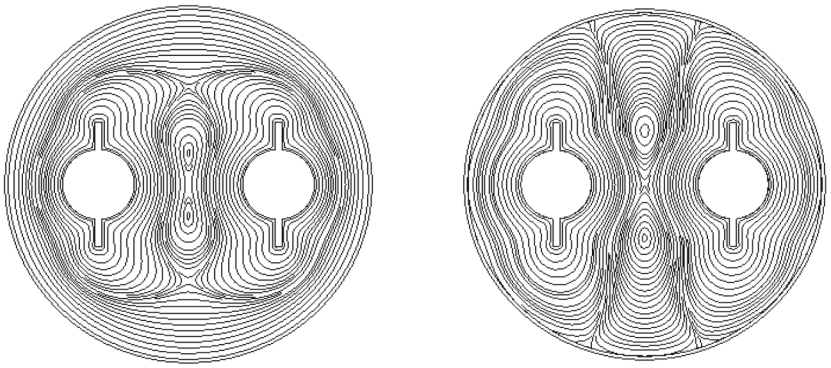

Configuration 2 : Rotating mixer with fins on the rods

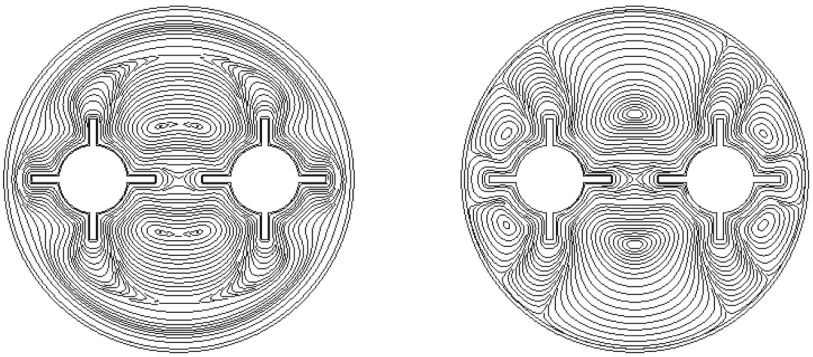

Configuration 3 : Rotating mixer with double fins on the rods

Fig. 11 Streamlines at $t = 4\ \tau$. Left side: for the continuous modulation protocol, Right side: for the alternative modulation protocol

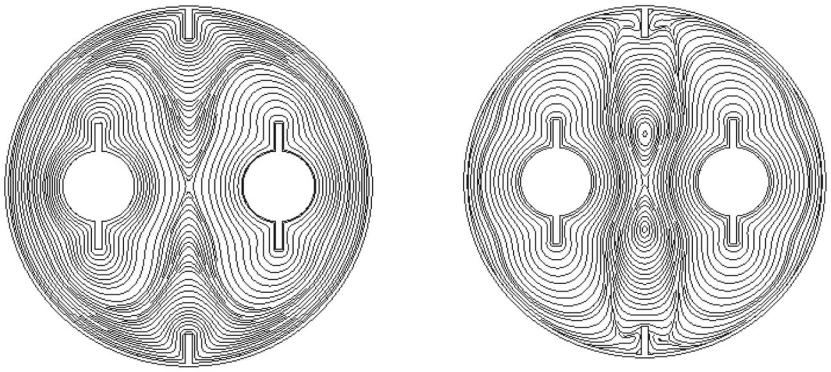

Configuration 4 : Rotating mixer with fins on the rods and on the tank

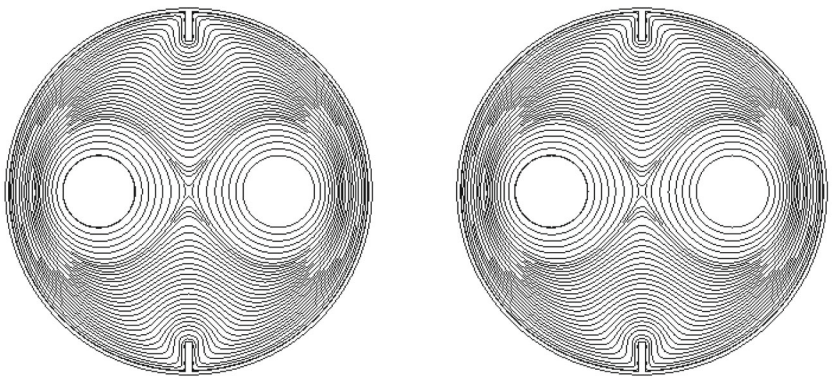

Configuration 5 : Rotating mixer with fins on the tank

Fig. 11 continued

6.1 Velocity profiles

Figures 5 and 6 present the two components of the velocity u and v generated by the two protocols, CM and ALT, in the two directions of the flow x and y for all the configurations considered at two instants 4τ and 4.5τ. As is known, these configurations are equipped with fins attached to the three compartments. This will destabilize the velocity profile in the dynamic boundary layers near the cylinder walls. Thus, we note that the unstationarity of the velocity field makes it possible to create permanent stresses which, by their role, improve the transfer phenomena. According to Figs. 5a and 6a, the velocity profiles are disturbed in both the CM and ALT protocols in configuration 3 mainly in the central area between the inner cylinders. Without the fins, the fluid in the central zone is almost immobile which prevents the fluid from moving toward the rest of the domain. This will create dead zones called islands. Note that the variation of the velocity profile retains its shape except in the case of configuration 3 where the velocity profile changes its evolution, in particular u as a function of y, see Figs. 5a, b, 6a, b.

6.2 Deformation and rotation rates

The term that creates both a non-integrable Navier–Stokes equation and twisted streamlines is the velocity gradient tensor $\overrightarrow{V}.\overline{\overline{\nabla}}\,\overrightarrow{V}$. It is composed of two tensors: the strain tensor and the rotation tensor. As much as these two quantities are important, the transfer phenomena such as heat and mass are considerable. The rotating rate generates transversal flows that mix the circulating fluids. While the fluids exposed to deformation processes are subjected to shear and elongation stresses of the fluid element. In addition, the combination of the two phenomena gives rise to complex behaviors of the velocity field, especially in 3D flows, called stretching and folding of vortices.

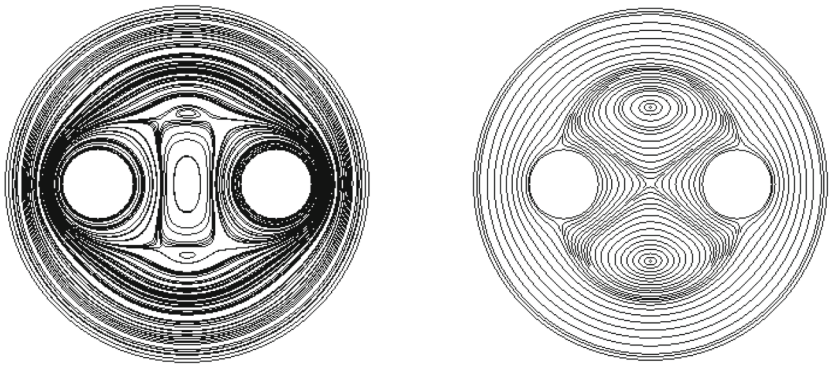

Configuration 1 : Rotating mixer without fins (base configuration)

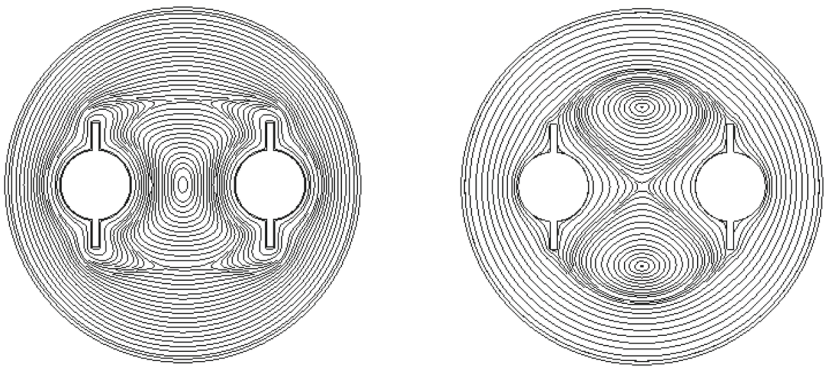

Configuration 2 : Rotating mixer with fins on the rods

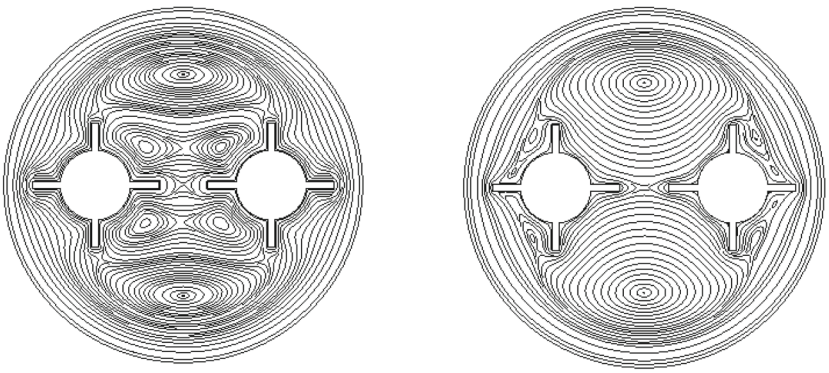

Configuration 3 : Rotating mixer with double fins on the rods

Fig. 12 Streamlines at $t = 4.5\ \tau$. Left side: for the continuous modulation protocol. Right side: for the alternative modulation protocol

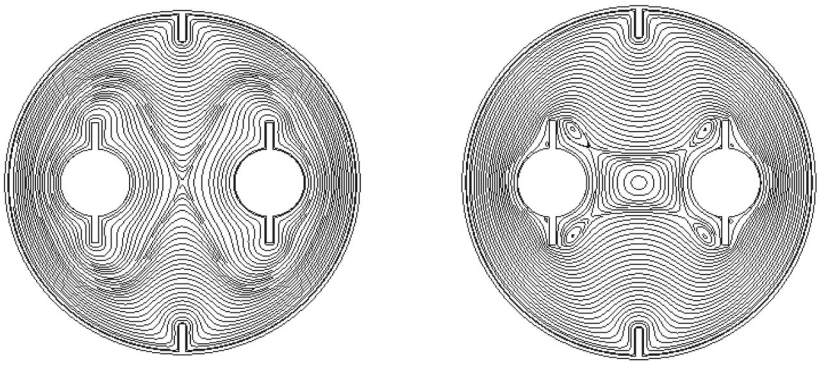

Configuration 4 : Rotating mixer with fins on the rods and on the tank

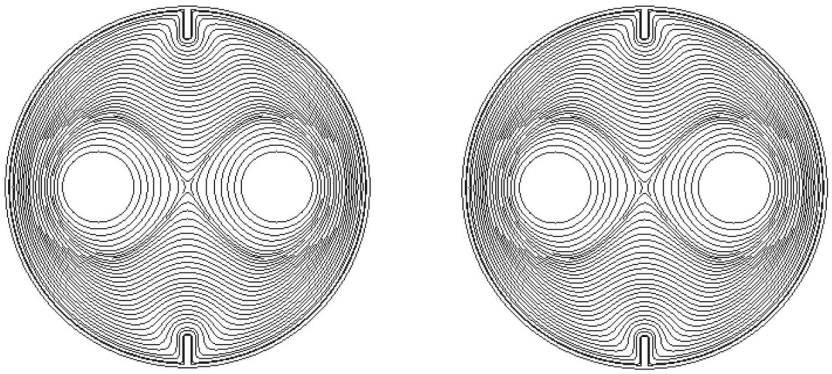

Configuration 5 : Rotating mixer with fins on the tank

Fig. 12 continued

Figures 7 and 8 present the evolutions of the deformation and rotation rates as function of the time engendered by the two protocols CM and ALT for all the configurations considered. Because the velocity field is periodic in time, the evolutions of these quantities keep the same temporal function. We point out that configuration 3 gives rise to higher deformation and rotation rates compared to the other configurations and this is achieved by the two protocols. Also, by a given protocol, the rate of deformation is better compared to the rate of rotation for a given configuration.

In configuration 3, the strain rates obtained by the CM and ALT protocols vary, respectively, between 0.3 and 0.35 and 0 and 0.3. The behavior of the rate of deformation is almost similar to that which characterizes the rate of deformation. These observations state that the CM protocol generates a higher strain and rotation rates compared to that created in the fluid by the ALT protocol.

6.3 Elongation rate

The elongation means the co-effect of the velocity field and the strain tensor. It contributed to stretching and folding the volume element in flow directions. This parameter generates secondary flows which improve the quality of the mixing. In addition, the oscillatory temporal velocity field creates intermittency movements, and by its role, it causes intense transfer phenomena. Positive elongation values show the process of stretching of the volume element, while negative values show the process of folding. This will make it possible to bring together in a fast and efficient way the zones of different distributions of the passive scalar (heat and mass).

Figure 9 and 10 present the evolutions of the elongation as function of the time in the considered configurations for two protocols CM and ALT, respectively. The basic configuration (1) presents weak elongation rates for the CM and ALT protocols in both directions (stretching and bending). This behavior makes this configuration less interesting. Note that configuration 5 has very high elongation rates compared to the other case studies in both agitation protocols ALT and CM. This property is the cause of the sensitivity to the initial

conditions of the equations system of the flow. In other words, two very close particles diverge exponentially over time, a very strong sign of the appearance of the chaotic advection.

6.4 Streamlines

Although streamlines present a qualitative indicator for describing flow, they reflect the complex behavior of fluid particles. They decipher the regular zones, dead zones, and complex zones of the flow. As we know, the addition of the fins to the walls makes the lines of currents more twisted compared to the basic cases where the walls of the tanks are without obstacles. To illustrate this behavior, Figs. 11 and 12 present the evolutions of the streamlines at different times in the considered configurations for two protocols, CM and ALT, respectively. It is remarkable that the fins considerably affect the shape of the streamlines by creating recirculation zones. On the one hand, these zones improve the dispersion of a passive scalar. On the other hand, the swirling agitation of the fluid accentuates the parietal friction which will allow the improvement of the parietal heat transfer. Configuration 3 shows an interesting performance compared to the other configurations with regard to the deformation of the streamlines. We also observe that the CM protocol is ahead of the ALT protocol in terms of flow complexity.

7 Conclusion and outlooks

In a previous study, El Omari and Le Guer [21] performed very interesting performances in terms of thermal mixing in the case of an unsteady two-dimensional flow. The used fluid is very viscous, where the Reynolds number is very low, and it is around 1.66. The main idea of our project is to mount fins on the walls of the tanks. These fins disturb the velocity field by creating recirculations in the flow. Created recirculations exhibit a static mixer that combines with temporal perturbations of the velocity field. Four configurations are tested by presenting the velocity profiles, the strain and rotation rates, the elongation rate, and the streamlines. All configurations assigned higher values to the local properties of the velocity field. Except for configuration 3, which appears to stand out from the other proposed cases. This is due to the arrangement of fins on the side walls of the inner cylinders, especially for the movement protocol, CM. Shear and rotation rates are significantly improved by configuration 3 of the CM protocol. The elongation process of a fluid element is calculated which is responsible of fluid stretching and bending. This phenomenon is known as Baker's transformation, where continuous application of this transformation mixes the fluids in such geometry. Consultation of the streamlines appeared in the considered configuration shows the formation of vortex zones, where streamlines intersect several times. This crossing displays the existence of hyperbolic points which characterize chaotic advection flow. Consequently, configuration 3 in the CM protocol can be chosen as the adequate mixer in industrial applications. Moreover, deformable fins can be an interesting alternative to increase mixing capacity in terms of quality and mixing time.

Authors' contribution TH and AL carried out the numerical results, and LY conceived of the presented idea. All authors contributed to the analysis of the results and to the writing of the manuscript.

Funding This paper received no specific grant from any funding agency.

Availability of data and materials This declaration is not applicable.

Declarations

Conflict of interest The authors have no competing interests to declare that are relevant to the content of this article.

Ethical approval This declaration is not applicable.

References

1. Metcalfe, G., Lester, D.: Mixing and heat transfer of highly viscous food products with a continuous chaotic duct flow. J. Food Eng. **95**(1), 21–29 (2009). https://doi.org/10.1016/j.jfoodeng.2009.04.032

2. Ali, N., Viggiano, B., Tutkun, M., Cal, R.B.: Forecasting the evolution of chaotic dynamics of two-phase slug flow regime. J. Pet. Sci. Eng. **205**, 108904 (2021). https://doi.org/10.1016/j.petrol.2021.108904
3. Molz, F., Faybishenko, B.: Increasing evidence for chaotic dynamics in the soil-plant-atmosphere system: a motivation for future research. Proc. Environ. Sci. **19**, 681–690 (2013). https://doi.org/10.1016/j.proenv.2013.06.077
4. Dias, R.C., Korhonen, O., Ketolainen, J., Lopes, J.A., Ervasti, T.: Flowsheet modelling of a powder continuous feeder-mixer system. Int. J. Pharm. **639**, 122969 (2023). https://doi.org/10.1016/j.ijpharm.2023.122969
5. Aref, H.: The development of chaotic advection. Phys. Fluids **14**(4), 1315–1325 (2002). https://doi.org/10.1063/1.1458932
6. Wang, W., Li, M., Xu, C.: Vertical chaotic mixing of oscillating feedback micromixer in passive mode. Chem. Eng. Sci. **263**, 118127 (2022). https://doi.org/10.1016/j.ces.2022.118127
7. Dai, X., et al.: Chaotic mixing properties under rotation plus revolution revealed by purification experiments and numerical simulations. J. Taiwan Inst. Chem. Eng. **142**, 104652 (2023). https://doi.org/10.1016/j.jtice.2022.104652
8. Younes, E., Moguen, Y., El Omari, K., Burghelea, T., Le Guer, Y., Castelain, C.: Experimental study of chaotic flow and mixing of Newtonian fluid in a rotating arc-wall mixer. Int. J. Heat Mass Transf. **187**, 122459 (2022). https://doi.org/10.1016/j.ijheatmasstransfer.2021.122459
9. Mouza, A.A., Patsa, C.M., Schönfeld, F.: Mixing performance of a chaotic micro-mixer. Chem. Eng. Res. Des. **86**(10), 1128–1134 (2008). https://doi.org/10.1016/j.cherd.2008.04.009
10. Lasbet, Y., Auvity, B., Castelain, C., Peerhossaini, H.: A chaotic heat-exchanger for PEMFC cooling applications. J. Power. Sources **156**, 114–118 (2006). https://doi.org/10.1016/j.jpowsour.2005.08.030
11. Revathi, R., Poornima, T.: Dynamics of stagnant Sutterby fluid due to mixed convection with an emphasis on thermal analysis. J. Therm. Anal. Calorim. (2024). https://doi.org/10.1007/s10973-024-12943-w
12. Malliswari, B., Poornima, T., Sreenivasulu, P., Bhaskar Reddy, N.: Electrical resistance heating distribution on three dimensional Jeffrey radiating nanofluid flow past stretching surface. J. Comput. Appl. Res. Mech. Eng., **11**(2), pp. 339–349 (2022). https://doi.org/10.22061/jcarme.2021.7013.1908.
13. Gunakala, S.R., Job, V.M., Nagarani, P., Sreenivasulu, P., Balkissoon, J.N.: Numerical study of unsteady mhd poiseuille flow with temperature-dependent viscosity through a porous channel under an oscillating pressure gradient. Palest. J. Math. **11**, 41–52 (2022)
14. Kunti, G., Bhattacharya, A., Chakraborty, S.: Analysis of micromixing of non-Newtonian fluids driven by alternating current electrothermal flow. J. Nonnewton. Fluid Mech. **247**, 123–131 (2017). https://doi.org/10.1016/j.jnnfm.2017.06.010
15. Lim, V., Hobby, A.M., McCarthy, M.J., McCarthy, K.L.: Laminar mixing of miscible fluids in a SMX mixer evaluated by magnetic resonance imaging (MRI). Chem. Eng. Sci. **137**, 1024–1033 (2015). https://doi.org/10.1016/j.ces.2015.07.003
16. Bai, C., Zhou, W., Yu, S., Zheng, T., Wang, C.: A surface acoustic wave-assisted micromixer with active temperature control. Sensors Actuat. A Phys. **346**, 113833 (2022). https://doi.org/10.1016/j.sna.2022.113833
17. Yuan, S., Jiang, B., Jiang, F., Drummer, D., Zhou, M.: international journal of heat and mass transfer numerical and experimental investigation of mixing enhancement in the passive planar mixer with bent baffles. Int. J. Heat Mass Transf. **191**, 122815 (2022). https://doi.org/10.1016/j.ijheatmasstransfer.2022.122815
18. Liao, W., Jing, D.: Experimental study on fluid mixing and pressure drop of mini-mixer with flexible vortex generator. Int. Commun. Heat Mass Transf. **142**, 106615 (2023). https://doi.org/10.1016/j.icheatmasstransfer.2023.106615
19. Amar, K., Embarek, D., Sofiane, K.: Chemical engineering research and design parametric study of the crossing elongation effect on the mixing performances using short two-layer crossing channels micromixer (TLCCM) geometry. Chem. Eng. Res. Des. **158**, 33–43 (2020). https://doi.org/10.1016/j.cherd.2020.03.010
20. Lasbet, Y., Aidaoui, L., Loubar, K.: Effects of the geometry scale on the behaviour of the local physical process of the velocity field in the laminar flow. Int. J. Heat Technol. **34**(3), 439–445 (2016). https://doi.org/10.18280/ijht.340313
21. El Omari, K., Le Guer, Y.: Thermal chaotic mixing of power-law fluids in a mixer with alternately rotating walls. J. Nonnewton. Fluid Mech. **165**(11–12), 641–651 (2010). https://doi.org/10.1016/j.jnnfm.2010.03.004
22. Msaad, A.A., et al.: Numerical simulation of thermal chaotic mixing in multiple rods rotating mixer. Case Stud. Therm. Eng. **10**(July), 388–398 (2017). https://doi.org/10.1016/j.csite.2017.09.005
23. Saatdjian, E., Rodrigo, A.J.S., Mota, J.P.B.: Stokes fl ow heat transfer in an annular, rotating heat exchanger. Appl. Therm. Eng. **31**(8–9), 1499–1507 (2011). https://doi.org/10.1016/j.applthermaleng.2011.01.037
24. El Omari, K., Le Guer, Y.: Alternate rotating walls for thermal chaotic mixing. Int. J. Heat Mass Transf. **53**(1–3), 123–134 (2010). https://doi.org/10.1016/j.ijheatmasstransfer.2009.09.046
25. Streeter, V.L., Wylie, E.B.: Fluid Mechanics (seventh edn.) (1979)
26. Khakhar, D.V., Ottino, J.M.: Deformation and breakup of slender drops in linear flows. J. Fluid Mech. **166**, 265–285 (1986). https://doi.org/10.1017/S0022112086000149